The Impact of *In Vivo* Reflectance Confocal Microscopy for the Diagnostic Accuracy of Melanoma and Equivocal Melanocytic Lesions

Giovanni Pellacani[1], Pascale Guitera[2], Caterina Longo[1], Michelle Avramidis[2], Stefania Seidenari[1] and Scott Menzies[2]

In vivo confocal reflectance microscopy recently showed promising results for melanoma (MM) diagnosis on a limited series. The aim of the study was to evaluate the sensitivity and specificity of confocal features for the diagnosis of MM 351 equivocal melanocytic lesions (136 MMs and 215 nevi) were evaluated for 37 confocal features by two blinded expert observers. χ^2 test, multivariate discriminant analysis and binary logistic regression were performed for the identification of the significant features and for testing newly created diagnostic models. Melanomas were mostly characterized by epidermal disarray and pagetoid cells in the epidermis, non-edged papillae, and cellular atypia at the junction, and atypical nests and bright nucleated cells in the upper dermis. On the other hand, regular dermal–epidermal architecture, and absence of pagetoid infiltration and atypical cells were suggestive of benign lesions. Five out of 136 melanomas, with mildly atypical melanocytes and occasional pagetoid cells at histopathology, were not diagnosed by confocal microscopy. Nevertheless, new diagnostic models showed no significant improvement compared with the previously proposed confocal microscopy algorithm. Owing to the visualization of cellular aspects, confocal microscopy seems useful for second level examination of clinically and dermoscopically equivocal lesions.

Journal of Investigative Dermatology (2007) **127,** 2759–2765; doi:10.1038/sj.jid.5700993; published online 26 July 2007

INTRODUCTION

In the previous decades cutaneous melanoma (MM) incidence increased by 3–7% annually in USA and Europe (Hall *et al.*, 1999; de Vries and Coebergh, 2004). The initial increase in mortality rate levelled off from the beginning of the 1990s (Bosetti *et al.*, 2004), in relation with particular efforts made for primary and secondary preventions by information campaigns and early diagnosis improvements (Koh *et al.*, 1995), which resulted in a constantly decreasing trend of melanoma thickness at diagnosis (Garbe *et al.*, 2000). The introduction and the worldwide diffusion of dermoscopy dramatically contributed to improve diagnostic accuracy for melanoma, especially for difficult-to-diagnose lesions (Pehamberger *et al.*, 1987; Argenziano *et al.*, 2003), although the not rare presence of featureless melanomas (Menzies *et al.*, 1996) and the increasing number of patients stimulated by prevention campaigns led to numerous unnecessary excisions (Del Mar *et al.*, 1997).

In vivo reflectance mode confocal microscopy (RCM) represents a novel technique, which offers the possibility to non-invasively examine the epidermis and the papillary dermis at a cellular resolution (Rajadhyaksha *et al.*, 1995). Some cytological and architectural aspects have been reported as suggestive of melanoma diagnosis (Langley *et al.*, 2001; Gerger *et al.*, 2005; Pellacani *et al.*, 2005a). We recently proposed an algorithm based on the identification of two major and four minor criteria, that seemed to improve diagnostic specificity for melanomas (Pellacani *et al.*, 2005b). The aim of this study was to define the impact of RCM features that distinguish melanomas and nevi, and to test newly created diagnostic models with standard statistical methods.

RESULTS

The list of the evaluated patterns is reported in Table 1. The relative and absolute frequencies, together with the odds ratio and 95% confidence interval (95% CI) values for the significant features, are reported in Table 2.

The presence of a marked epidermal disarray was more frequently observed in melanomas (Figure 1a), although present in one-third of nevi, whereas homogeneous epidermis, characterized by regular honeycombed and/or cobble-

[1]*Department of Dermatology, University of Modena and Reggio Emilia, Modena, Italy and* [2]*Faculty of Medicine, Sydney Melanoma Diagnostic Centre, Sydney Cancer Centre and Dermatology Department, Royal Prince Alfred Hospital, University of Sydney, Sydney, New South Wales, Australia*

The work was performed in Sydney, Australia, and Modena, Italy.

Correspondence: Professor Giovanni Pellacani, Department of Dermatology, University of Modena and Reggio Emilia, Via del Pozzo 71, Modena 41100, Italy. E-mail: pellacani.giovanni@unimo.it

Abbreviations: AUC, area under the curve; 95% CI, 95% confidence interval; RCM, in vivo *reflectance confocal microscopy; ROC, receiver operating characteristic*

Received 24 January 2007; revised 8 May 2007; accepted 29 May 2007; published online 26 July 2007

© 2007 The Society for Investigative Dermatology

Table 1. List and description of the RCM features evaluated for melanocytic lesion diagnosis

RCM features	
Suprabasal epidermis	
Regular honeycombed pattern	Structure formed by 10–20 μm polygonal cells with dark nuclei and bright thin cytoplasm
Regular cobblestone pattern	Structure consisting of small polygonal cells with very bright cytoplasm separated by a less bright border
Atypical honeycombed pattern	Irregularity in size of the cells and thickness of the contour within a honeycombed structure (Figure S1)
Atypical cobblestone pattern	Irregularity in size and/or refractivity of the cells within a cobblestone structure (Figure S1)
Atypical cobblestone pattern with small nucleated cells	Presence of numerous cells with visible nuclei within a cobblestone structure
Epidermal disarray	Disarray of the normal architecture of the superficial layers with unevenly distributed bright granular particles and cells, in the absence of honeycombed or cobblestone pattern
Grainy image	Bright granular dust-like particles barely discernible as individual granules
Roundish pagetoid cells	Large roundish nucleated cells, with a dark nucleus and bright cytoplasm, within suprabasal layers
Dendritic pagetoid cells	Bright nucleated cells with dendritic-like branches within suprabasal layers
Number of pagetoid cells	Number of clearly visible pagetoid cells evaluated on five samples of 0.5×0.5 mm image
Size of pagetoid cells	Mean size of the cellular body of clearly visible pagetoid cells evaluated on five samples of 0.5×0.5 mm image
Pleomorphic pagetoid infiltration	Variability of the aspect of pagetoid cells
Widespread pagetoid infiltration	Presence of pagetoid cells throughout the explored lesion area
Dermal epidermal junction	
Edged papillae	Dermal papillae surrounded by a rim of bright cells, appearing as bright rings sharply contrasting with the dark background
Non-edged papillae	Dermal papillae without a demarcated rim of bright cells, but separated by a series of large reflecting cells
Presence of large visible cells	Large (at least twice the size of normal keratinocytes) bright nucleated cells within the basal layer
Non-pleomorphic	Monomorphous cells
Mild cellular atypia	Irregular larger cells sporadically visible within typical cell architecture
Marked cellular atypia	Irregular in size, shape, and reflectivity, round to oval or stellate, occasionally with branching dendritic-like structures, distributed throughout the lesion
Number of large cells	Number of clearly visible large cells evaluated on five samples of 0.5×0.5 mm image
Junctional nests	Presence of clusters of reflecting cells in contiguity with the basal layer
Junctional clusters	Oval compact cellular aggregates bulging within the dermal papilla, directly in connection with the basal cell layer
Junctional thickenings	Enlargements of the inter-papillary space formed by aggregated cells
Cells in sheet-like structures	Cells in the transition of the epidermis and dermis not aggregated in clusters but closely distributed in the same plane with the loss of dermal papillae
Non-pleomorphic cells	Roundish regularly shaped cells.
Pleomorphic roundish cells	Cells with irregular shape and/or reflectivity
Pleomorphic spindled cells	Elongated cells oriented toward the same direction.
Upper dermis	
Regular dense nests	Compact aggregates with sharp margin and similar cells in morphology and refractivity
Atypical nests	Cell aggregates with irregular shape, reflectivity and/or morphology of the structure and/or the cells
Non-homogeneous nests	A mixed dense and sparse cell aggregates showing non homogeneity in cell morphology and reflectivity
Sparse cell nests	Irregularly aggregated and sparse cells individually visible, confined within a darker well-demarcated area
Cerebriform nests	Confluent amorphous aggregates of low reflecting cells exhibiting granular cytoplasm without evident nuclei and ill defined borders, being the aggregates brain-like with fine hyporeflective ''fissures'' like appearance.
Nucleated cells within the papilla	Round to oval or triangular cells with well-demarcated bright cytoplasm and well-demarcated dark nucleus infiltrating dermal papilla
Bright small cells and/or hyper-reflecting spots	Small hypereflective dots and small cells with very bright cytoplasm
Plump bright cells	Plump irregularly shaped bright cells with ill-defined borders and usually no visible nucleus, sometimes crowded within the papilla
Reticulated fibers	Elongated fibrillar structures (1–5 μm) without cellular component distributed side by side throughout the dermis
Broadened reticulated fibers	Web-like structures of fibrillae larger than 5 μm
Thick cordons	Bunch of amorphous or fibrillar structures gathered into large fasciae

RCM, *in vivo* reflectance confocal microscopy.

Table 2. The RCM features discriminating melanomas and nevi ($P<0.05$)

RCM features	136 melanomas (%)	215 Nevi (%)	OR (95% CI)[1]	Standardized discriminant analysis coefficients	Binary logistic regression coefficients
Superficial layers					
Regular honeycombed and/or cobblestone pattern	17 (12.5)	112 (52.1)	0.131 (0.074–0.233)		
Epidermal disarray	85 (62.5)	72 (33.5)	3.310 (2.115–5.181)	0.332	
Roundish pagetoid cells	106 (77.9)	40 (18.6)	15.458 (9.087–26.296)	0.620	1.747
Dendritic pagetoid cells	75 (55.1)	48 (22.3)	4.278 (2.684–6.817)		
More than 3 pagetoid cells in 5 0.5×0.5 mm images	110 (80.9)	51 (23.7)	13.605 (8.004–23.125)		
Pagetoid cells larger than 20 μm	110 (80.9)	59 (27.4)	11.186 (6.638–18.852)		
Pleomorphic pagetoid infiltration	74 (54.4)	25 (11.6)	9.071 (5.305–15.510)	0.208	0.836
Widespread pagetoid infiltration	48 (35.3)	18 (8.37)	5.970 (3.285–10.846)		
Dermal epidermal junction					
Edged papillae	61 (44.9)	181 (84.2)	0.153 (0.093–0.251)		
Non-edged papillae	122 (89.7)	89 (41.4)	12.337 (6.663–22.843)	0.488	1.56
Mild to marked cellular atypia	100 (73.5)	58 (26.9)	7.519 (4.627–12.219)		
Cells in sheet-like structures	24 (17.6)	4 (1.9)	11.30 (3.827–33.386)		
Junctional nests	57 (41.9)	130 (60.5)	0.472 (0.305–0.730)	−0.203	
Junctional clusters	17 (12.5)	60 (27.9)	0.369 (0.205–0.665)		
Junctional thickenings	56 (41.2)	122 (56.7)	0.534 (0.345–0.825)		
Upper dermis					
Dense nests	49 (36.0)	103 (47.9)	0.612 (0.394–0.952)		−0.895
Atypical nests	72 (52.9)	56 (26.0)	3.194 (2.028–5.029)		
Non-homogeneous nests	60 (44.1)	43 (20)	3.158 (1.962–5.081)		0.824
Sparse cell nests	24 (17.6)	15 (6.9)	2.857 (1.439–5.669)		
Cerebriform nests	11 (8.1)	4 (1.9)	4.642 (1.447–14.890)		
Nucleated cells within the papilla	65 (47.8)	27 (12.5)	6.374 (3.769–10.778)	0.265	

95% CI, 95% confidence interval; OR, odds ratio; RCM, *in vivo* reflectance confocal microscopy.
OR and 95% CI for melanomas.

stone pattern, was strongly related to benign lesions (Figure 2a). Pagetoid infiltration constituted by roundish cells was reported in 78% of melanomas and 19% of nevi, whereas the observation of dendritic pagetoid cells, although significant, had a relatively lower odds ratio for melanomas. More than three cells per image and the presence of cells larger than 20 μm were predominantly observed in melanomas. Pleomorphism and widespread diffusion throughout the lesion of pagetoid cells were specific but not sensitive markers of malignancy.

At the dermo–epidermal junction level, non-edged papillae were observed in 90% of melanomas and in 41% of nevi, whereas edged papillae were predominantly present in nevi. Mild to marked atypia was observed in 73 and 27% of melanomas and nevi, respectively. Cells distributed in sheet-like structures, disrupting the papillary architecture of the basal layer (Figure 1b), were highly specific, but with low sensitivity for melanoma. On the other hand, junctional nests, both clusters and thickenings, were characteristic for benign lesions (Figure 2b).

Immediately below the dermal epidermal junction, cells aggregated in nests were visible in over the half of lesions. Whereas regular dense nests were significantly more represented in nevi (Figure 2c), the presence of atypical nests, such as the non-homogeneous nests (Figure 1c), sparse cell nests, and/or cerebriform ones, correlated with malignancy (53% of melanomas), although reported also in 26% of nevi. Within the dermal papilla almost half of the melanomas showed large nucleated cells, compared with 13% of nevi. No difference in the frequency of plump bright cells ($P=0.217$), bright small cells, and/or hyper-reflecting spots ($P=0.524$), and broadened reticulated and/or large bundles of fibers ($P=0.609$) was reported within the two groups (data not shown).

Comparing equal or thinner than 1 mm melanomas and thicker ones, epidermal disarray, cells in sheet-like structures, cerebriform nests and nucleated cells within dermal papilla were significantly associated with thick melanomas. The total number of positive variables slightly correlated with Breslow's thickness (Pearson $r=0.290$, $P=0.001$), showing less

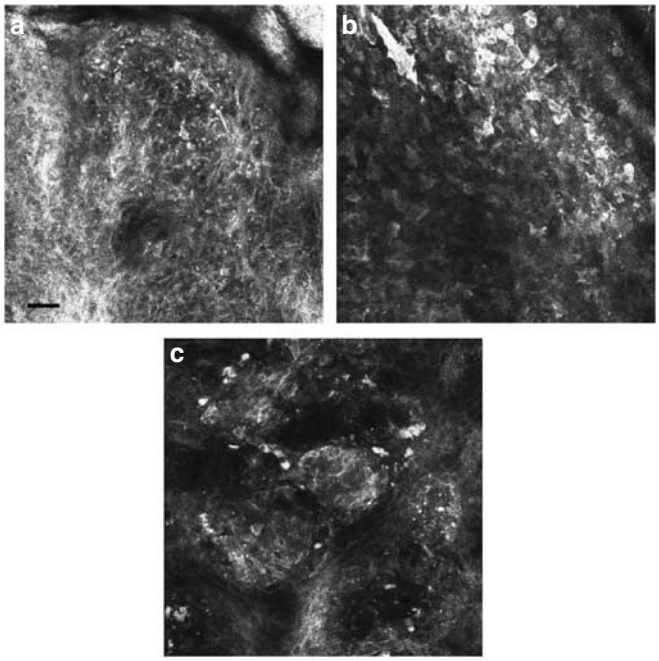

Figure 1. *In vivo* confocal microscopic features characteristic for melanomas. (**a**) Suprabasal epidermis disarray, with unevenly distributed bright granular particles and pagetoid cells; (**b**) atypical cells in sheet-like structures at the dermal–epidermal junction; (**c**) non-homogeneous nests, constituted by aggregates of mixed dense and sparse cell. Bar = 50 μm.

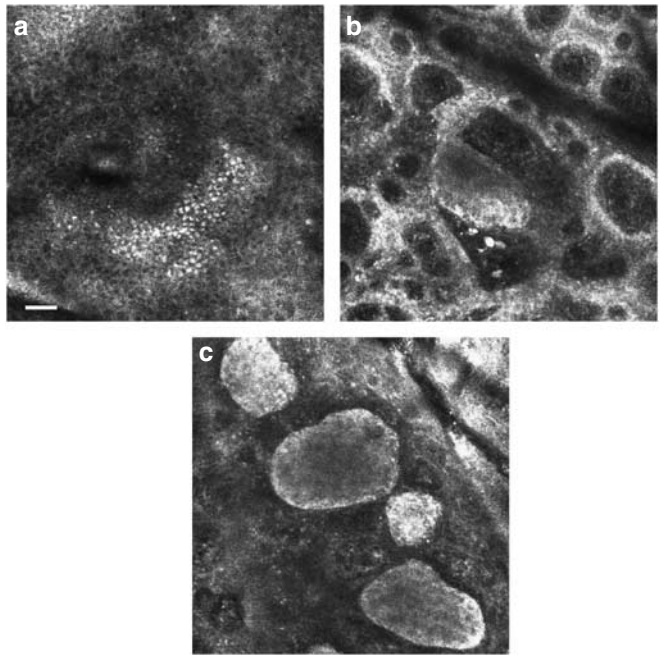

Figure 2. *In vivo* confocal microscopic features characteristic for nevi. (**a**) Regular honeycombed and cobblestone pattern; (**b**) regular junctional nests of cells (junctional cluster and junctional thickening); (**c**) regular dense nests in the dermis. Bar = 50 μm.

positive variables in thin melanomas (median 7, interquartile range 5–9), compared with thicker ones (median 10, interquartile range 7–10) ($P = 0.005$).

The sample was split at random into two equal parts, a training set and a test set. Analysis of the training set showed that six features were independently correlated with malignancy by means of discriminant analysis, corresponding to, in order of relevance, roundish pagetoid cells, non-edged papillae, epidermal disarray, nucleated cells in the dermal papilla, and pleomorphic pagetoid infiltration as positive features and junctional nests as negative, whereas binary logistic regression confirmed roundish pagetoid cells, non-edged papillae and pleomorphic pagetoid infiltration, with the inclusion of dishomogeneous nests as positive feature and dense nests as negative one (Table 2).

The models selected and estimated from the training set by means of discriminant analysis and binary logistic regression were used for prediction on the test set, showing in receiver operating characteristic (ROC) analysis an area under the curve (AUC) of 0.833 (95% CI 0.771–0.895) and 0.827 (95% CI 0.765–0.890), respectively, both resulting slightly inferior to the previously proposed RCM algorithm score (Pellacani *et al.*, 2005b), tested on the same population (AUC of 0.852; 95% CI 0.795–0.910) (Figure 3).

On the whole study sample, the RCM score algorithm showed its best sensitivity for a score equal or greater than 2 (96.3%), with a 52.1% specificity, whereas five out of 136 melanomas (3.7%) were completely lacking positive features (RCM score = 0). The previously proposed threshold of three was confirmed as the most accurate one for the RCM score algorithm, with 78.1% of correct diagnoses, corresponding to 91.9% sensitivity and 69.3% specificity (Table 3).

DISCUSSION

As its recent beginning, RCM appeared promising for melanoma diagnosis (Langley *et al.*, 2001; Busam *et al.*, 2002; Gerger *et al.*, 2005, 2006; Pellacani *et al.*, 2005b;). On two series of pigmented skin lesions, both including 27 melanomas and a large proportion of clearly benign nevi, the sensitivity and specificity for melanoma diagnosis, obtained from the evaluations of a few selected images per case, was close to perfection (Gerger *et al.*, 2005, 2006). Recently, we examined a series of equivocal melanocytic lesions, including 37 melanomas and 65 nevi, all excised because of dermoscopic aspects suggestive of malignancy, and an algorithm based on the detection of six features was developed (Pellacani *et al.*, 2005b).

This study setting was developed on a large series of cases and the evaluation of each was performed in a complete blind setting to avoid evaluation bias. In our series, many RCM features statistically differed between melanomas and nevi. The presence of an epidermal disarray, previously reported by others as characteristic for melanoma (Langley *et al.*, 2001), but not relevant in our previous series (Pellacani *et al.*, 2005b), was statistically significant and independently correlated with malignancy (Figure 1a). On the other hand, regular epidermal architecture, showing a cobblestone and/or honeycombed pattern, seemed to be specific for benign lesions (Figure 2a). Moreover, this study highlighted the importance of the identification of pagetoid infiltration that

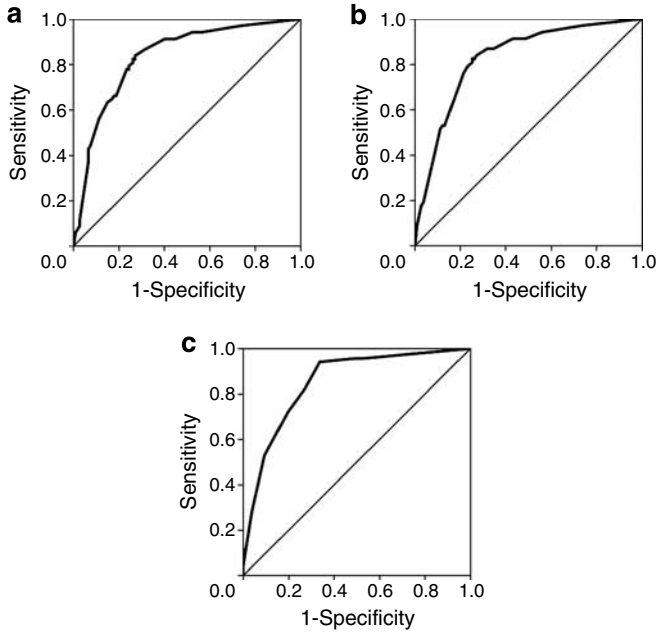

Figure 3. Model selection and estimation used only the training set, whereas ROC analysis used only the test set. (**a**) ROC curve obtained by means of discriminant analysis (AUC = 0.833); (**b**) ROC curve from binary logistic regression (AUC = 0.827); (**c**) ROC curve from RCM score algorithm (AUC = 0.852).

resulted the most relevant discriminating parameter. A lesion showing roundish pagetoid cells had a 15 times greater risk to be malignant. Melanomas tend to have disarranged dermo–epidermal junction architecture, corresponding to non-edged papillae and atypical cells, sometimes forming sheet-like structures (Figure 1b). The presence of atypical nests and/or nucleated cells in the dermis (Figure 1c) were characteristic for melanomas, whereas benign lesions more frequently showed regular rete-ridges, corresponding to edged papillae at RCM, and regular nests of cells in the dermal–epidermal junction (Figure 2b) and in the dermis (Figure 2c), although the specificity of the latter features was not high.

Melanomas thicker than 1 mm usually showed numerous positive features compared with thinner ones, frequently presenting a marked disarray of the epidermis, in association with disarrangement of the dermal–epidermal architecture and dermal infiltration of malignant cells, as shown by atypical melanocytic cells in sheet like structures, infiltrating dermal papilla and/or clustered in cerebriform nests.

Another aim of this study was to test the diagnostic accuracy of RCM in very difficult melanocytic lesions, that underwent excision for the presence of dermoscopic features of melanoma (72% of cases) or following changes after sequential digital monitoring (28%). Although numerous features were statistically significant, any attempt to create a new model for melanoma discrimination failed, obtaining in ROC analysis a diagnostic discriminating power similar to the RCM score that achieved a 96% sensitivity and a specificity of 52% for a threshold equal or greater than 2 and 92% sensitivity and 69% specificity for a score equal or greater than 3.

Table 3. Sensitivity and specificity for RCM score with different thresholds

RCM score thresholds[1]	Sensitivity	Specificity
⩾1	96.3	49.3
⩾2	96.3	52.1
⩾3	91.9	69.3
⩾4	79.4	77.2
⩾5	66.9	82.3
⩾6	49.3	91.6
⩾7	23.5	98.1
⩾8	2.2	100

RCM, *in vivo* reflectance confocal microscopy.
[1]Total RCM score, (non-edged papillae)*2+(mild to marked cell atypia)*2+(roundish pagetoid cells)+(widespread pagetoid infiltration)+(cerebriform nests)+(nucleated cells in the dermis).

In conclusion, RCM seemed useful for the accurate identification of melanocytic lesions, proving to enable the correct diagnosis of the majority of melanomas and of a significant proportion of moderately atypical nevi. As approximately 5–10 minutes are needed for the complete exploration of a single lesion, the device appears particularly functional for second level examination of equivocal lesions selected by clinical and dermoscopic evaluation, aiming to reduce the number of unnecessary excisions without reducing the sensitivity. However, a follow-up should be considered for lesions lacking RCM atypical features, owing to the low probability, but not impossibility, of false negative melanoma. In fact, in our series, five out of 136 melanomas showed an RCM score equal to 0, corresponding at histopathology to *in situ* lesions in three cases, and 0.3 and 0.5 mm in the others, all showing histopathologically a predominantly nested proliferation with mildly atypical melanocytes and occasional pagetoid cells, suggesting that lesions with few and occasional diagnostic clues may be underestimated by RCM. Nevertheless, giving real-time reliable diagnostic information, RCM represents a relevant method to aid in the decision-making process facing difficult lesions.

MATERIALS AND METHODS

The study has been approved by the authors' Institutional Review Board, and the Declaration of Helsinki Principles were followed. Participants gave their written informed consent.

Study sample

This study sample included a total of 351 melanocytic lesions from 332 patients (158 female and 174 males, median age of 47.7, interquartile range 35.9–60.4), of which 136 were melanomas, 215 were melanocytic nevi (49 junctional, 132 compound, nine intradermal and 25 Spitz nevi), recorded by means of RCM at the Sydney Melanoma Diagnostic Centre of the Royal Prince Alfred Hospital, University of Sydney, (156 lesions) and at the Department of Dermatology of the University of Modena and Reggio Emilia (195

lesions). The lesions were located on the head/neck region in 15 cases, on the abdomen and chest in 68, on the back in 135, on the upper limbs in 50, and on the lower limbs in 83, without significant differences between the site distribution of melanomas and nevi ($P=0.07$). All lesions excised to exclude melanoma, based upon dermoscopy, sequential digital monitoring, or history of change in standard clinical practice, were included. No lesions excised for cosmetic reasons or solely due to a patient request were included. Of the 136 melanomas, 42 were *in situ*, 86 were superficial spreading, and eight nodular, with a median Breslow's thickness of 0.49 mm (interquartile range: 0–0.89 mm). Of the invasive melanomas, 66% ($n=62$) were <1 mm Breslow's thickness, 25 % ($n=23$) were 1.01 to 2.0 mm thick, and 9% ($n=8$) were 2.01 to 4.0 mm. Lentigo maligna and lesions of palms and soles were not included in the study on clinical and histopathologic grounds.

Instruments and acquisition procedure

Before biopsy, RCM images were acquired by means of near-infrared reflectance confocal laser scanning microscopes (Vivascope 1000® and Vivascope 1500®, Lucid Inc., Henrietta, New York), which employs an 830 nm laser beam with a maximum power of 35 mW. Instrument and acquisition procedures are described elsewhere (Rajadhyaksha *et al.*, 1999). Each image corresponds to a horizontal section at a selected depth with an approximately 0.5×0.5 mm field of view, and a lateral resolution of 1.0 μm and axial resolution of 3–5 μm (Rajadhyaksha *et al.*, 1999). A sequence of montage images (''block'' images) were acquired for each lesion at the level of the dermo-epidermal junction to explore a 4×4 mm field of view per lesion. For large lesions, not completely comprised within the field of view, the device was centered on the lesion or on the portion with the most suspicious dermoscopic features, according to pattern analysis and standard second step melanoma diagnostic methods (Argenziano *et al.*, 2003). Confocal sections, beginning at the stratum corneum and ending inside the papillary dermis, were recorded at areas of interest. More than 100 capture images per lesion were recorded.

RCM feature description

RCM features were described by two expert observers (GP from the University of Modena for the evaluation of the Sydney cases, and PG from Sydney for the evaluation of the Modena ones), blinded from anamnestic information, dermoscopy, and clinical aspects, but not for the location and the patient's age. In detail, each observer evaluated the images previously acquired by the other, opening codified folders containing all the images acquired for the corresponding case and a file for location and the patient's age. At the end of the study, the patients' codes were broken and the evaluations were matched with the histologic diagnoses for statistical analysis.

The single features were previously discussed on sample cases not included in the study sample, as published elsewhere (Pellacani *et al.*, 2005b). A series of 37 features, corresponding to previous observations (Busam *et al.*, 2001, 2002; Langley *et al.*, 2001; Gerger *et al.*, 2005; Marghoob *et al.*, 2005; Pellacani *et al* 2005a, b, c, d) and some new descriptors, have been considered at three different depth levels (Table 1). All the features were evaluated for the presence/absence (binary non-parametric data), with the exception of the number and size of pagetoid cells that were dichotomized for statistics considering the presence of more than three pagetoid cells in five 0.5×0.5 mm images and pagetoid cells larger than 20 μm, respectively.

The total RCM score was also calculated for each lesion evaluating the presence of two major features (non-edged papillae and cellular atypia at dermal–epidermal junction), each scored two points, and four minor ones (roundish pagetoid cells, widespread pagetoid infiltration, cerebriform nests, nucleated cells within the papilla), each scored 1 point (Pellacani *et al.*, 2005b), and compared with new models obtained by statistical analysis.

Statistics

Statistical evaluation was carried out employing the SPSS statistical package (release 12.0. 0, 2003; SPSS Inc., Chicago, IL). Absolute and relative frequencies of the observations in benign and malignant lesions were obtained for each RCM feature. Significant differences between melanomas and benign lesions, and between equal or thinner than 1 mm melanomas and thicker ones, were evaluated by means of the χ^2 test of independence (Fisher's exact test was applied if any expected cell value in the 2×2 table was less than 5). Moreover, the median and the interquartile range of the number of the identified positive features were calculated for melanomas equal or thinner that 1 mm and for thicker ones, and compared by Mann–Whitney test. Correlation between the total number of positive features and Breslow's thickness was tested according with Pearson. For an estimate of melanoma risk, a calculation of the odds ratio and 95% CI was performed. Sensitivity, specificity, positive and negative predictive value and odds ratio + 95% CI were calculated for each RCM score value (ranging from 0 to 8). For multivariate analysis, the study sample was randomly divided into a training set and a test set, each comprising 50% of the lesions. Multivariate discriminant analysis and binary logistic regression were performed for the identification of the independently significant features and for the validation of the efficacy of RCM in distinguishing between benign and malignant lesions. Logistic regression and discriminant analysis are useful for predicting the presence or absence of a characteristic or outcome based on values of a set of predictor variables, similarly to linear regression model but suited to models where the dependent variable is dichotomous. Stepwise forward selection was used to choose the features for the prediction model. Goodness-of-fit statistics and Wilk's lambda were used to determine whether the models adequately described the data for logistic regression and discriminant analysis, respectively. At each step, the predictor with the largest score statistic whose significance value is less than the default value of 0.05 for logistic regression and the largest F to Enter value that exceeds the entry criteria (by default, 3.84) for discriminant analysis, were added to the models. Variables with score statistic value greater than 0.05 and with F to Enter values smaller than 3.84, respectively, were left out the models. ROC analysis was performed to investigate sensitivity and specificity of the discriminant analysis and binary logistic regression equations, and for the RCM score (Hanley and McNeil, 1982). The AUC, which represents an index of the overall discriminant power, was calculated by the non-parametric trapezoidal method. The final chosen model along with its parameter estimates were then used for prediction and estimation of the AUC in test set. A *P*-value less than 0.05 was considered significant.

CONFLICT OF INTEREST

The authors state no conflict of interest.

ACKNOWLEDGMENTS

This study was partially supported by grants from the Fondazione Cassa di Risparmio di Modena, Italy, the CNR (Centro Nazionale per la Ricerca), Italy, and the Cancer Institute New South Wales, Sydney, Australia.

SUPPLEMENTARY MATERIAL

Figure S1. Irregular but not completely disarranged epidermis as observed by *in vivo* confocal microscopy.

REFERENCES

Argenziano G, Soyer HP, Chimenti S, Talamini R, Corona R, Sera F *et al.* (2003) Dermoscopy of pigmented skin lesions: results of a consensus meeting via the internet. *J Am Acad Dermatol* 48:679–93

Bosetti C, La Vecchia C, Naldi L, Lucchini F, Negri E, Levi F (2004) Mortality from cutaneous malignant melanoma in Europe. Has the epidemic levelled off? *Melanoma Res* 14:301–9

Busam KJ, Charles C, Lee G, Halpern AC (2001) Morphological features of melanocytes, pigmented keratinocytes, and melanophages by *in vivo* confocal scanning laser microscopy. *Mod Pathol* 14:862–8

Busam KJ, Charles C, Lohmann CM, Marghoob A, Goldgeier M, Halpern AC (2002) Detection of intraepidermal malignant melanoma *in vivo* by confocal scanning laser microscopy. *Melanoma Res* 12:349–55

de Vries E, Coebergh JW (2004) Cutaneous malignant melanoma in Europe. *Eu J Cancer* 40:2355–66

Del Mar CB, Green AC, Battistutta D (1997) Do public media campaigns designed to increase skin cancer awareness result in increased skin excision rates? *Aust N Z J Public Health* 21:751–4

Garbe C, McLeod GR, Buettner PG (2000) Time trends of cutaneous melanoma in Queensland, Australia and Central Europe. *Cancer* 89:1269–78

Gerger A, Koller S, Kern T, Massone C, Steiger K, Richtig E *et al.* (2005) Diagnostic applicability of *in vivo* confocal laser scanning microscopy in melanocytic skin tumors. *J Invest Dermatol* 124:493–8

Gerger A, Koller S, Weger W, Richtig E, Kerl H, Samonigg H *et al.* (2006) Sensitivity and specificity of confocal laser-scanning microscopy for *in vivo* diagnosis of malignant skin tumors. *Cancer* 107:193–200

Hall HL, Miller DR, Rogers JD, Bewerse B (1999) Update on the incidence and mortality from melanoma in the United States. *J Am Acad Dermatol* 9:178–82

Hanley JA, McNeil BJ (1982) The meaning and use of the area under a receiver operating characteristic (ROC) curve. *Radiology* 143:29–36

Koh HK, Geller AC, Miller DR, Lew RA (1995) The early detection of and screening for melanoma. International status. *Cancer* 75:674–83

Langley RGB, Rajadhyaksha M, Dwyer PJ, Sober AJ, Flotte TJ, Anderson RR (2001) Confocal scanning laser microscopy of benign and malignant melanocytic skin lesions *in vivo*. *J Am Acad Dermatol* 45:365–76

Marghoob AA, Charles CA, Busam KJ, Rajadhyaksha M, Lee G, Clark-Loeser L *et al.* (2005) *In vivo* confocal scanning laser microscopy of a series of congenital melanocytic nevi suggestive of having developed malignant melanoma. *Arch Dermatol* 141:1401–12

Menzies SW, Ingvar C, Crotty KA, McCarthy WH (1996) Frequency and morphologic characteristics of invasive melanomas lacking specific surface macroscopic features. *Arch Dermatol* 132:1178–82

Pehamberger H, Steiner A, Wolff K (1987) *In vivo* epiluminescence microscopy of pigmented skin lesions. I. Pattern analysis of pigmented skin lesions. *J Am Acad Dermatol* 17:571–83

Pellacani G, Cesinaro AM, Longo C, Grana C, Seidenari S (2005c) Microscopic *in vivo* description of cellular architecture of dermoscopic pigment network in nevi and melanomas. *Arch Dermatol* 141:147–54

Pellacani G, Cesinaro AM, Seidenari S (2005a) Reflectance-mode confocal microscopy for the *in vivo* characterization of pagetoid melanocytosis in melanomas and nevi. *J Invest Dermatol* 125:532–7

Pellacani G, Cesinaro AM, Seidenari S (2005b) Reflectance-mode confocal microscopy of pigmented skin lesions-improvement in melanoma diagnostic specificity. *J Am Acad Dermatol* 53:979–85

Pellacani G, Cesinaro AM, Seidenari S (2005d) *In vivo* assessment of melanocytic nests in nevi and melanomas by reflectance confocal microscopy. *Mod Pathol* 18:469–74

Rajadhyaksha M, Gonzalez S, Zavislan JM, Anderson RR, Webb RH (1999) *In vivo* confocal scanning laser microscopy of human skin II: advances in instrumentation and comparison with histology. *J Invest Dermatol* 113:293–303

Rajadhyaksha M, Grossman M, Esterowitz D, Webb RH, Anderson RR (1995) *In vivo* confocal scanning laser microscopy of human skin: melanin provides strong contrast. *J Invest Dermatol* 104:946–52